

Snow evolution in Sierra Nevada (Spain) from an energy balance model validated with Landsat TM data

Javier Herrero*^a, María J. Polo^b, Miguel A. Losada, M.A.^c

^a Fluvial Dynamics and Hydrology Research Group, University of Granada. Edf. CEAMA. Av. del Mediterráneo s/n. 18071. Granada. Spain.

^b Fluvial Dynamics and Hydrology Research Group, University of Córdoba. Campus de Rabanales, Edificio Leonardo Da Vinci, Área de Ingeniería Hidráulica, 14071 Córdoba, Spain.

^c Environmental Flows Dynamics Research Group, University of Granada. Edf. CEAMA. Granada. Spain.

ABSTRACT

Sierra Nevada Mountains are the highest continental altitude in Spain. Located in the South, facing the Mediterranean Sea in a distance of less than 40 km, the high level of solar energy income throughout the year, together with the extremely variable character of climate in such latitudes, make it necessary to use energy balance approaches to characterize the snow cover evolution. Wind and relative humidity become decisive factors in the evolution of the snow cover due to the high evaporation rates that can arise under favourable meteorological conditions. This work presents the enhanced capability of the combination of Landsat TM data with the simulation of an energy balance model to produce sequences of hourly high resolution maps of snow cover and depth distribution under variable meteorological conditions such as those found in Mediterranean mountainous watersheds. Despite the good agreement found between observed and predicted snow pixels, different examples of disagreement arose in the boundaries, most of them related to the temperature and wind speed spatial pattern simulation together with the discrimination between rain and snowfall occurrence.

Keywords: Snow, modelling, Landsat, Mediterranean, snow cover

1. INTRODUCTION

The snow associated with high mountain zones in warm or semiarid climates has a special relevance in terms of management, as water normally becomes a basic resource for the development of these regions. The snow reduces the direct runoff and feeds the aquifers during the spring and early summer. This supply of water at the beginning of the dry season, where precipitation tends to be scarce, diminishes the severity of the droughts.

Satellite remote sensing of the snow started decades ago, particularly dealing with the evolution of the areal extent of snow cover¹. Beyond the measurement of the evolution of the snow extension, other properties such as albedo, grain size, percentage of each pixel actually covered by snow and even water equivalent and snow depth can be deduced from the analysis of these images^{2,3,4,5}. This was possible thanks to the more sophisticated multi-spectral sensors, although also more limited and expensive. But if we want to make use of the extensive dataset available from the most popular satellites like NOAA/AVHRR, EOS/MODIS or Landsat, only snow cover surface can be readily measured.

* herrero@ugr.es; phone: 0034 958241000 – ext 31163; www.ugr.es/~herrero

A physically-based distributed hydrological model applies input meteorological data through different physical and hydrological properties of soil and its cover to simulate the surface component of the water cycle (see ⁶). Its results can be directly applied to management studies or can serve as a starting point for other studies and modelling based on water, such as those regarding ecology, sediment or water quality. The simulation of the snow inside these models is based on the mass and energy balance in the snowpack^{7,8,9}. This balance keeps track of snow accumulation and of its subsequent metamorphism, including melting and evaporation¹⁰. They simulate at a temporal scale under the hour and at a spatial scale within meters. This means that their results can be easily related to satellite images. This is a mutual interaction, as satellite data can be used for the calibration or correction of the snow extension simulated with a physical model. On the other hand, the model can be used to interpolate or simulate the evolution of the snow cover between two measured images at a higher temporal resolution and preserving the physical sense of the processes generating that variation. The model is also able to extend the satellite information regarding extension of snow to thickness or total water hold in the snowpack in a direct and easy way.

The calibration of a distributed physically-based snow model demands accurate spatial information. Nevertheless, the temporal continuity of this information is not such a demanding aspect. Thus, Landsat 5 TM and Landsat 7 ETM+ imagery, with a 30 m spatial resolution every 16 alternate days for each satellite, 8 days considering both, become an adequate set to be used in this task. Landsat images will allow the calibration and validation of the distributed model in key dates distributed throughout the different stages of accumulation and melting of the snow cover.

2. LOCATION

The Sierra Nevada Mountains are located in Southern Spain at latitude 37° N. They form a lineal mountain range 60 km long, parallel to the shore line of the Mediterranean Sea (see Fig. 1). This is only 35 km from the mountain crests, whose peaks have a maximum altitude of 3480 m. Because of this altitude, the mountains are covered with snow during the spring and winter months despite the warm Mediterranean climate in the surrounding areas. There is snow at altitudes greater than 2000 m in Sierra Nevada Natural Park (Fig. 1), which extends over a total area of 1750 km². Climate and weather conditions are so varied that five different climates coexist in the 5 basins that drain the mountain range. These climates range from Alpine to semi-arid Mediterranean and to tropical.

Precipitation is distributed heterogeneously throughout the region due to the shadow effects produced by the orography. The slope facing southwards has slightly lower precipitation rates and receives a greater amount of solar radiation. Between 1990 and 2006, average annual precipitation was 550 mm, unevenly distributed between 350 mm of the nearby semiarid areas and 900 mm of the mountain peaks. Variability between years is also remarkable: in Refugio Poqueira Station, at 2500 m.a.s.l, the gauged precipitation varied from 434 mm in 2005 to 1516 mm in 2010¹¹. Minimum temperatures in the mountainous area are as low as -20° C at certain times in the winter, even though the average annual temperature is never less than 0° C even at the highest altitudes. Periods of mild temperatures during winter are usual, causing several snowmelt cycles during the snow season.

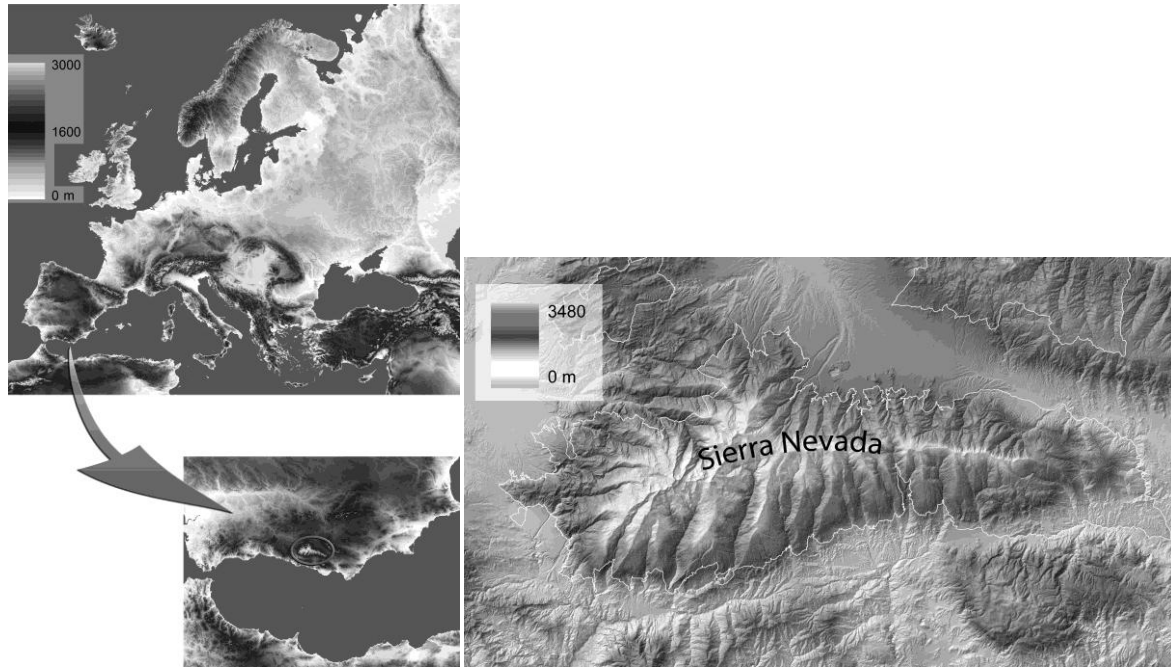


Figure 1. Location of Sierra Nevada Mountains. The white line represents the limits of Sierra Nevada National Park.

3. SNOW MODEL

The whole region of Sierra Nevada National Park was simulated with the hydrological model WiMMed^{12,13}. The model solves the mass and the energy balance of the snowpack in order to calculate snow accumulation, sublimation, condensation and snow melt. As a result, the value of the state variables of the snow cover (snow water equivalent, density and internal energy) or the derived variables (thickness and temperature) can be obtained as distributed maps at an hourly scale. Further details on the characteristics of the snow model can be found in Herrero et al., 2009¹⁴. The model requires the following meteorological data: daily and hourly total precipitation, daily maximum and minimum temperature, daily solar radiation, mean daily longwave radiation, mean daily wind speed and mean daily vapour pressure. The model deals with some meteorological data at a daily scale, so it is possible to include the large amount of weather stations that work at this frequency. The model distributes these records at an hourly scale through temporal interpolations specific for every meteorological variable which depends on its properties¹⁵. The spatial scale selected for the simulations is 30x30 meters, in such a way that it matches Landsat resolution. This facilitates the comparison between model results and the snow cover distribution maps extracted from the satellite images. Besides the snow cover area, maps of thickness and accumulated water in the snow will be obtained from the model results.

4. SNOW IN LANDSAT SCENE

The classification of a pixel as snow or snow-free in a satellite multi-spectral image is based on the particular properties of the snow reflectance: very high at visible and very low at near-infrared spectrum (1.6 μm). Fig. 2 shows 3 bands of the Landsat TM-5 image on the 25th of November of 2002 in the vicinity of Sierra Nevada. Snow and clouds have a similar reflectance in the visible region (Fig. 2.a and 2.b), but snow virtually disappears in Landsat band 5 (Fig 2.c) centered at 1.6 μm . Landsat bands 1 and 2 in this regions are saturated, which makes it difficult to study the snow albedo (shortwave reflectance).

Landsat scenes are previously processed for geometric, atmospheric and radiometric correction, explained in detail in Díaz, 2007¹⁶. In the visible bands of a Landsat scene, snow can almost be discriminated visually from white bodies such as clear nude rocks, greenhouses, buildings or, above all, clouds, based on their different textures. But if we want to use a numerical methodology for the discrimination of snow cover, combined analysis of these bands together with band 5 are necessary. In this sense, the use of the Snow Index SI⁴ and the Normalized Difference Snow Index¹⁷ becomes helpful (see Fig 2.d). SI and NDSI are defined as:

$$SI = TM2 - TM5 \quad (1)$$

$$NDSI = (TM2 - TM5) / (TM2 + TM5) \quad (2)$$

where TM_i refers to the reflectance value in the band i of the Landsat image. Using these two indexes, together with the ratio TM₅/TM₂, the normalized band 1 TM₁/Σ TM_i and the value in bands TM₁ and TM₄ directly, Rosenthal and Dozier⁴ developed a series of complex decision trees to discriminate snow in a satellite image with a precision comparable to that obtained with high resolution airborne photography. This methodology was applied in another Sierra Nevada (California), but as the calibrated coefficients depend on the lithology, vegetation and illumination, in principle, it is restricted to the calibrated region. Alternatively, Dozier & Painter⁵ present a simple criterion for snow detection: a pixel in a clear area is covered by the snow if NDSI > 0.4 and TM₄ > 0.11, whereas in a forested area the condition becomes 0.1 < NDSI < 0.4.

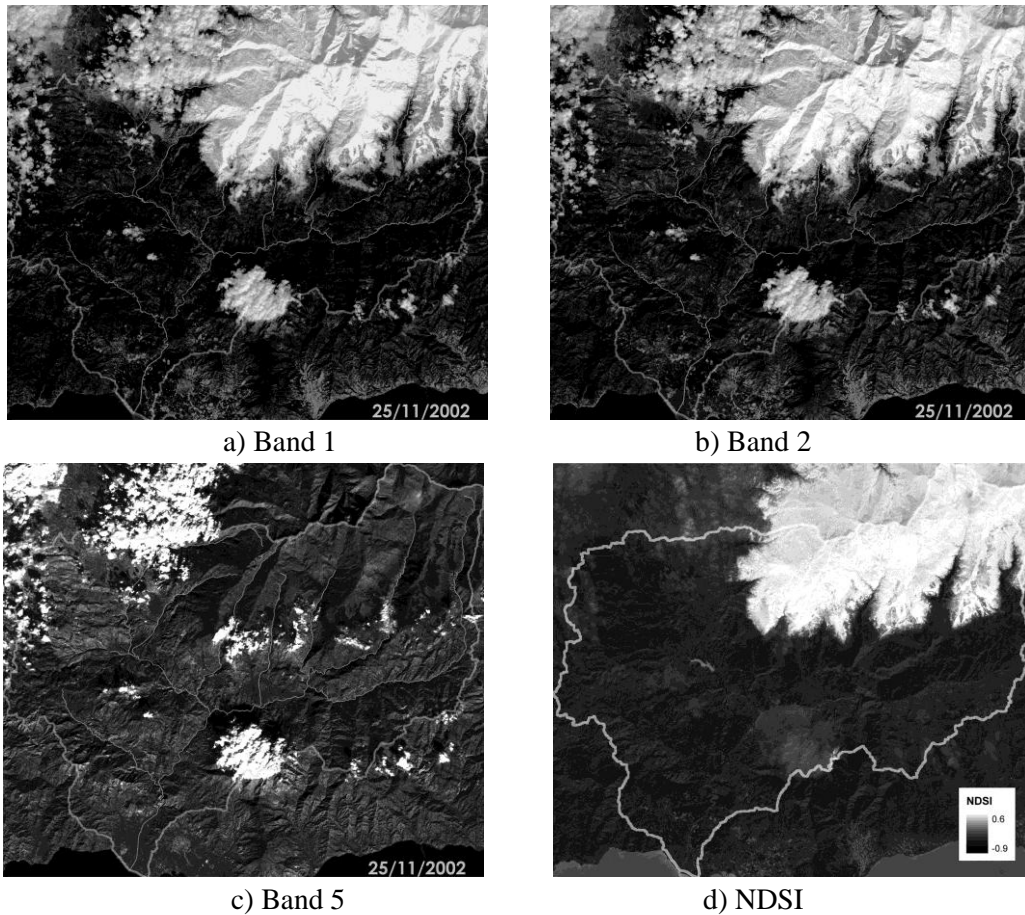


Figure 2. Bands 1, 2 and 5 of the Landsat-5 TM image and NDSI index.

Herrero¹⁸ performed several analyses on those indexes and ratios in the Guadalfeo river basin, which contains a major part of Sierra Nevada (Spain), in order to discriminate snow cover in the Landsat images. In this study, NDSI was found to be a significantly better predictor than SI. As a result, a methodology for snow classification in this area was established. Those pixels where $NDSI > 0.15$ and $TM1 > 0.06$ are classified as snow. Additionally, a threshold with the minimum elevation with snow presence, inferred from the elevation vs. percentage of snow graph, is used to eliminate some misclassified pixels. From the remaining pixels, those where $NDSI > 0.28$ and $TM > 0.1$ are classified as unsolved, a category that mainly contains pixels with patchy snow on the edges of the snow cover.

5. COMPARISON SATELLITE DATA-MODEL ESTIMATIONS

The success of the simulation of the snow is evaluated through the comparison between the estimated snow cover maps corresponding in date and time to every available Landsat image. In the pixel to pixel comparison, 4 different combinations are possible:

- Measured pixel with snow and simulated pixel with snow $P_{m, s}$
- Measured pixel without snow and simulated pixel without snow $P_{no-m, no-s}$
- Measured pixel with snow and simulated pixel without snow $P_{m, no-s}$
- Measured pixel without snow and simulated pixel with snow $P_{no-m, s}$

$P_{m, s}$ and $P_{no-m, no-s}$ refer to pixels correctly reproduced by the model, while $P_{m, no-s}$ and $P_{no-m, s}$ indicate, respectively, the under and overestimation of the simulated snow area. The number of pixels included in every category indicates the goodness of each fit. In order to have more direct and meaningful indicators, we defined three dimensionless parameters, obtained by the combination of previous parameters:

- Total surface fit index TSFI over the whole number of pixels in the image P_{Tot}
 - $TSFI = (P_{m, s} + P_{no-m, no-s}) / P_{Tot}$
- Snow-covered surface fit index SSFI over the active pixels, that is, over those pixels with measured or simulated snow P_{Snow} .
 - $SSFI = P_{m, s} / P_{Snow} = P_{m, s} / (P_{Tot} - P_{no-m, no-s})$
- Balance of the SSFI, B_{SSFI}
 - $B_{SSFI} = (P_{no-m, s} - P_{m, no-s}) / (P_{m, no-s} + P_{no-m, s})$

TSFI and SSFI will reach 1 for a perfect fit and 0 for the worst possible estimation. $P_{m, s}$ and $P_{no-m, no-s}$ are of equal worth in TSFI, as both values refer to successful pixel estimations. But for those cases when one of both parameters prevailed upon the other, this index may not be meaningful. That is the reason why SSFI is defined by taking into account only those pixels with measured or simulated snow. A low value of this index indicates disagreement because of the presence of $P_{m, no-s}$, $P_{no-m, s}$ or both. BSSFI helps us to distinguish between these three situations, as a 0 value of this parameter indicates even failures of under and overestimation on the snow simulated by the model. Positive values up to 1 are caused by overestimation, while negative values down to -1 indicate underestimation.

6. RESULTS AND DISCUSSION

Two complete hydrological years for calibration and validation were used. A model simulation of the snow was run from the beginning of the year, and compared to several Landsat images at their corresponding date, without any intermediate correction of the modelling. SSFI index reached a mean value of 0.7 for the 9 images analyzed during calibration and validation, ranging from 0.84 to 0.53. B_{SSFI} index was very variable between -0.98 and 0.88, denoting that there is not any tendency in the model to overestimate or underestimate snow cover.

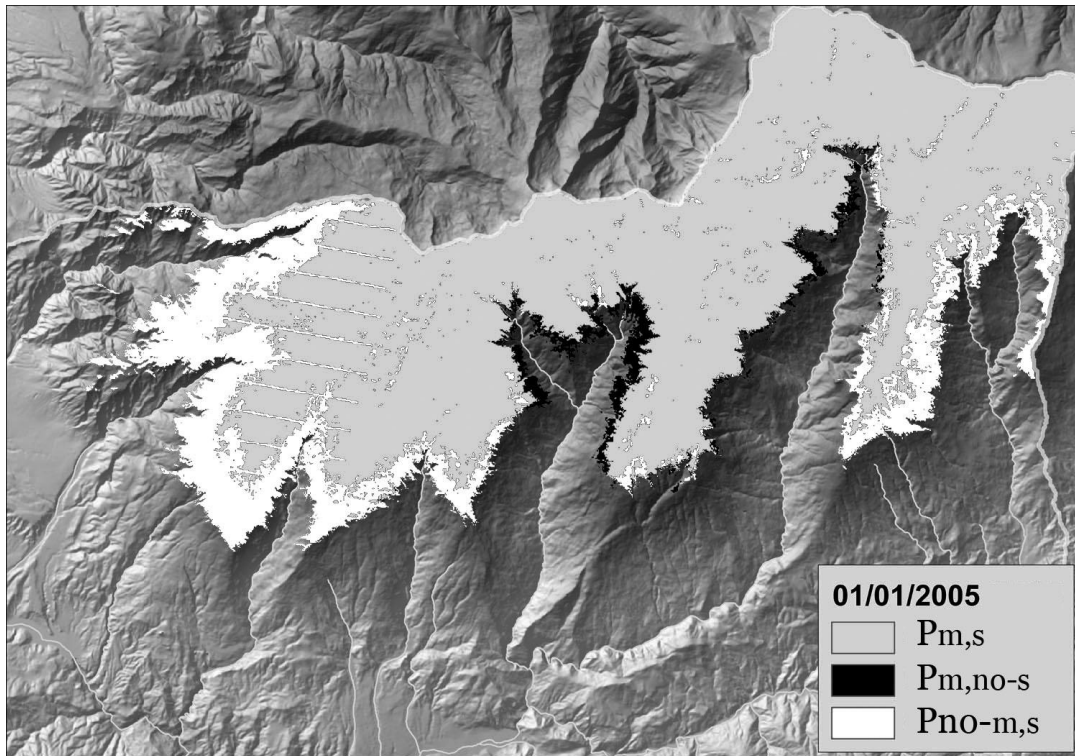


Figure 3. Example of compared measured and simulated snow cover.

Most of the disagreements between measurement and simulation are due to the meteorological input data and not to the resolution of the model itself. Two critical moments were detected: 1) accumulation periods, when the influence of temperature is crucial to determining snowfall in each pixel and 2) periods with enhanced snowmelt or evaporation from the snow due to high wind speeds. In case 1, minor differences in the estimation of hourly temperature and precipitation can lead to great differences in the snow covered area. To overcome this problem, a denser meteorological network with at least hourly data would be needed. The main difficulty in case 2 is the accurate representation of changes in the wind speed because of the rough orography. This means that the snow modelling in high mountain demands an advanced model for wind speed interpolation adapted to complex terrain. In both cases, when meteorological conditions are stabilized and snowmelt has persistently affected the snowpack, the snow cover area is accurately represented by the model, that is, modelling and measurements become synchronized again.

7. CONCLUSIONS

Satellite images are a very direct and spatially precise source of data about snow cover extension. Combined with a distributed physically-based snow model, they can provide the information needed for the model calibration, in order to estimate not only the presence of snow, but also the thickness or the amount of water contained in the snowpack. Also, the model can be used as a physically-based tool for the interpolation of the snow cover between images.

In the modelling of a Mediterranean mountainous region, where snow is very dynamic as it is subjected to constant changes in areal extension, WiMMed hydrological model succeeds in simulating the snow behaviour, with an overall fit of 0.7 in SSFI index. Major discrepancies arose because of the insufficient meteorological data in space and frequency of the measurements, mainly temperature during snowfalls and high wind speeds. An improvement of the wind speed interpolator model, with a better performance under complex terrain circumstances, would also be desirable, as the influence of this variable over snow cover extension, especially in warm climates, is outstanding.

REFERENCES

- [1] Rango, A. and Itten, K. I., "Satellite potentials in snowcover monitoring and runoff prediction", *Nordic Hydrol.*, 7, 209-230 (1976).
- [2] Dozier, J., Schneider, S. R. and McGinnis, D. F., "Effect of grain size and snowpack water equivalence on visible and near-infrared satellite observations of snow", *Wat. Res. Res.*, 17, 1213-1221, (1981).
- [3] Hall, D.K., Riggs, G.A. and Salomonson, V.V., "Development of methods for mapping global snow cover using moderate resolution imaging spectroradiometer data", *Remote Sensing of Environment* 54, 127-140, (1995).
- [4] Rosenthal, W. and Dozier, J., "Automated mapping of montane snow cover at subpixel resolution from Landsat Thematic Mapper", *Wat. Res. Res.* 32(1), 115-130, (1996).
- [5] Dozier, J. and Painter, T., "Multispectral and hyperspectral remote sensing of alpine snow properties", *Annual Review of Earth and Planetary Science* 32, 465-494, (2004).
- [6] Dingman, L., [Physical Hydrology. 2nd edition], Prentice Hall, New York, (2002).
- [7] Anderson, E.A., "Development and testing of snow pack energy balance equations", *Wat. Res. Res.* 4(1), 19-37, (1968).
- [8] Jordan, R., [A one-dimensional temperature model for a snow cover.], CRREL Special Report 91-16, US Army Corps of Engineers, Cold Regions Research & Engineering Laboratory. Hanover, New Hampshire, USA, (1991)
- [9] Tarboton, D.G. and Luce, C.H. [Utah Energy Balance Snow Accumulation and Melt Model (UEB), Computer model technical description and users guide], Utah Water Research Laboratory and USDA Forest Service Intermountain Research Station, (1996).
- [10] Armstrong, R.L. and Brun, E., [Snow and climate: physical processes, surface energy exchange and modeling], Cambridge University Press, UK, (2008).
- [11] Herrero, J., Aguilar, C., Millares, A., Moñino, A., Polo, M.J. and Losada, M.A., "Mediterranean high mountain meteorology from continuous data obtained by a permanent meteorological station at Sierra Nevada, Spain", *Proc. EGU General Assembly 2011*. Vienna, Austria, (2011).
- [12] Herrero, J., Aguilar, C., Millares, A., Egüén, M., Carpintero, M., Polo and M.J., Losada, M. [WiMMed. User Manual v1.1], Grupo de Dinámica Fluvial e Hidrología de la Universidad de Córdoba y Grupo de Dinámica de Flujos Ambientales de la Universidad de Granada, Spain, (2010).

- [13] Polo, M.J., Herrero, J., Aguilar, C., Millares, A., Moñino, A., Nieto, S. and Losada, M.A., "WiMMed, a distributed physically-based watershed model (I): Description and validation", in *Environmental Hydraulics: Theoretical, Experimental & Computational Solutions*. CRC Press/Balkema. 225-228, (2009).
- [14] Herrero J., Polo, M.J., Moñino, A. and Losada, M.A., "An energy balance snowmelt model in a Mediterranean site", *J. Hydrol.* 371, pp. 98-107, (2009).
- [15] Herrero, J., Aguilar, C., Polo, M.J. and Losada, M.A., "Mapping of meteorological variables for runoff generation forecast in distributed hydrological modeling" , *Proc. Hydraulic measurements and Experimental Methods*, New York, 606-611, (2007).
- [16] Díaz, A. [Series temporales de vegetación para un modelo hidrológico distribuido], *Monografías 2007*, Grupo de Hidrología e Hidráulica Agrícola, Universidad de Córdoba, Spain, (2007).
- [17] Dozier, J., "Spectral signature of alpine snow cover from the Landsat Thematic Mapper", *Rem. Sens. Env.* 28, 9-22 (1989).
- [18] Herrero, J., "Modelo físico de acumulación y fusión de la nieve. Aplicación a Sierra Nevada (España).", Thesis dissertation, Grupo de Dinámica de Flujos Ambientales de la Universidad de Granada, Spain, (2007).